Reduction of the Peak SAR in the Human Head With Metamaterials

Jiunn-Nan Hwang and Fu-Chiarng Chen

Abstract—The electromagnetic interaction between the antenna and the human head is reduced with metamaterials. Preliminary study of SAR reduction with metamaterials is performed by the finite-difference time-domain method with lossy Drude model. It is found that the specific absorption rate (SAR) in the head can be reduced by placing the metamaterials between the antenna and the head. The antenna performances and radiation pattern with metamaterials are analyzed. A comparative study with other SAR reduction techniques is also provided. The metamaterials can be obtained by arranging split ring resonators (SRRs) periodically. In this research, we design the SRRs operated at 900 and 1800 MHz bands. The design procedure will be described. Numerical results of the SAR values in a muscle cube with the presence of SRRs are shown to validate the effect of SAR reduction. These results can provide helpful information in designing the mobile communication equipments for safety compliance.

Index Terms—Metamaterials, lossy drude model, specific absorption rate (SAR), split ring resonators (SRRs).

I. INTRODUCTION

THE use of the cellular phones has been growing rapidly in the global communities. The absorption of electromagnetic (EM) energy emitted from cellular phone has been discussed in recent years. Exposure guidelines for protecting the human body from EM exposure have been issued in many countries. The specific absorption rate (SAR) is a defined parameter for evaluating power deposition in human tissue. For the cellular phone compliance, the SAR value must not exceed the exposure guidelines [1], [2]. Some numerical results have implied that the peak 1 g averaged SAR value (SAR_{1g}) may exceed the exposure guidelines when a portable telephone is placed extremely close to the head [3], [4]. Therefore, many researchers are working on reducing the SAR values. In [5], a ferrite sheet was proposed to use as a protection attachment between the antenna and a head. It was found that a ferrite sheet can result in SAR reduction and the radiation pattern of the antenna can be less affected. In [6], a perfect electric conductor (PEC) reflector was arranged between a human head and the driver of a folded loop antenna. Numerical results showed that the radiation efficiency can be enhanced and the peak SAR value can be reduced. In [7], a study on the effects of attaching conductive materials

to cellular phone for SAR reduction has been presented. It indicated that the position of the shielding material is an important factor for SAR reduction effectiveness.

Recently, metamaterials have inspired great interests due to their unique physical properties and novel application [8], [9]. Metamaterials denote artificially constructed materials having electromagnetic properties not generally found in nature. Two important parameters, electric permittivity and magnetic permeability determine the response of the materials to the electromagnetic propagation. Mediums with negative permittivity can be obtained by arranging the metallic thin wires periodically [10]. On the other hand, an array of split ring resonators (SRRs) can exhibit negative effective permeability [11]. The metallic thin wires and SRRs are narrow-banded and lossy materials. When one of the effective medium parameters is negative and the other is positive, the medium will display a stop band. The metamaterials is on a scale less than the wavelength of radiation and uses low density of metal. The structures are resonant due to internal capacitance and inductance. The stop band of metamaterials can be designed at operation bands of cellular phone while the size of metamaterials is similar to that of cellular phone. In [12], the designed SRRs operated at 1.8 GHz were used to reduce the SAR value in a lossy material. The metamaterials are designed on circuit board so it may be easily integrated to the cellular phone. Simulation of wave propagation into metamaterials was proposed in [13]. The authors developed the finite-difference time-domain (FDTD) method with lossy Drude models for metamaterials simulation. This method is a useful approach to study the wave propagation characteristics of metamaterials [14] and has been further developed with the perfectly matched layer and extended to three-dimension problem [15].

In this paper, the metamaterials are used for SAR reduction. An anatomically based human head model and a dipole antenna are assumed. The metamaterials are placed between the antenna and a human head. Preliminary study of SAR reduction with metamaterials is performed by 3-D FDTD method with lossy Drude model. In order to study SAR reduction of antenna operated at the GSM 900 band, the effective medium parameter of metamaterials is set to be negative at 900 MHz. Different positions, sizes, and negative medium parameters of metamaterials for SAR reduction effectiveness are also analyzed. To investigate the influence of metamaterials on the antenna, the peak SAR_{1g} and antenna performances are demonstrated. The use of metamaterials is also compared with other SAR reduction techniques. We design the metamaterials from periodically arrangement of SRRs. By properly designing structure parameters of SRRs, the effective medium parameter can be negative around 900 and 1800 MHz bands. The SAR value in a simplified
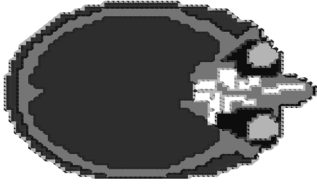
Fig. 1. Human head model for FDTD computation.

muscle cube with the presence of SRRs is studied. Numerical results are demonstrated to validate the effect of SAR reduction with metamaterials.

II. PRELIMINARY STUDIES OF SAR REDUCTION BY FDTD METHOD WITH LOSSY DRUDE MODEL

A. FDTD Method With Lossy Drude Model

Preliminary studies of SAR reduction with metamaterials were performed by FDTD with lossy Drude model in this section. The SAR reduction effectiveness and antenna performance with different positions, sizes, and negative medium parameters of metamaterials will be analyzed. The head model used in this study was obtained from MRI-based head model through The Whole Brain Atlas[1] website. Six types of tissues, i.e., bone, brain, muscle, eyeball, fat, and skin, were involved in this model. Fig. 1 shows a horizontal cross section through the eyes of this head model. The electrical properties of tissues were taken from [3], [4].

Numerical simulation of SAR value was performed by FDTD method. The parameters for FDTD computation were as follows. The simulated domain were $128 \times 128 \times 128$ cells. The cell sizes were set as $\Delta x = \Delta y = \Delta z = 3.0$ mm. The computational domain was terminated with 8 cells PML. A dipole antenna was modeled by thin-wire approximation. The formulation of SAR is defined as $\mathrm{SAR} = \sigma |E|^2 / 2\rho$, where E, σ and ρ are the electric field, conductivity, and mass density in the head, respectively.

Simulations of metamaterials are performed by FDTD method with lossy Drude model. The method is a useful method to understand the wave propagation characteristics of metamaterials. In this method, let μ and ε be modeled by the following expressions

$$\varepsilon = \varepsilon_0 \left(1 - \frac{\omega_{\mathrm{pe}}^2}{\omega(\omega + i\Gamma_e)} \right) \tag{1}$$

$$\mu = \mu_0 \left(1 - \frac{\omega_{\mathrm{pm}}^2}{\omega(\omega + i\Gamma_m)} \right) \tag{2}$$

where ω_p and Γ denote the corresponding plasma and damping frequencies, respectively.

We can provide a slight variation of (1) as

$$\varepsilon = \varepsilon_0 \left(1 - \frac{\omega_{\mathrm{pe}}^2}{(\omega + i\Gamma_{e1})(\omega + i\Gamma_{e1})} \right). \tag{3}$$
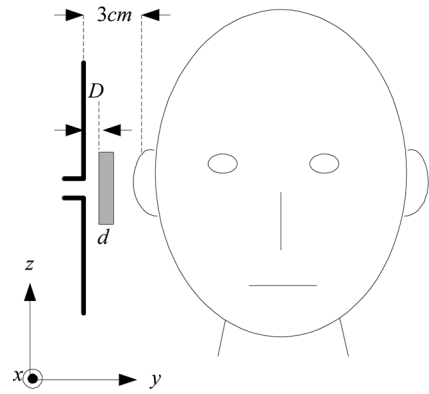
[1]http://www.med.harvard.edu/AANLIB/home.html

Fig. 2. The head and antenna models for SAR calculation.

Frequency	Tissue	[3]	[4]	This work
900MHz	Whole head	2.17	2.28	2.43

This model is actually Lorentz medium model, e.g.

$$\varepsilon_L = \varepsilon_0 \left(1 - \frac{\omega_{\mathrm{pe}}^2}{\omega^2 + i\Gamma_e\omega - \omega_{0e}^2} \right) \tag{4}$$

where $\Gamma_e = \Gamma_{e1} + \Gamma_{e2}$ and $\omega_{0e}^2 = \Gamma_{e1}\Gamma_{e2}$.

With this method, we can treat the metamaterials as homogenous materials with frequency-dispersive material parameters.

B. SAR Calculation in the Head With Metamaterials

Fig. 2 shows the human head and antenna models in this study. The antenna was arranged parallel to the head axis. The distance between the antenna and head surface was 3.0 cm. The SAR value was calculated for an antenna output power equal to 600 mW. The calculated peak SAR_{1g} without metamaterials was 2.43 W/kg. The SAR simulation is compared with the results in [3], [4] for validation, as shown in Table I. Although different head and antenna models were used, the simulated SAR_{1g} is similar to their results.

The metamaterials were placed between the antenna and human head. The distance D between the antenna feeding point and edge of metamaterials was 3 mm. The size of metamaterials in xz plane was 45 mm $\times$ 45 mm and thickness d was 6 mm.

The SAR value and antenna performance with metamaterials were analyzed. To evaluate the power radiated from the antenna, the source impedance (Z_S) was assumed equal to the complex conjugate of the free space radiation impedance $(Z_S = 102.14 - j83.78 \ \Omega)$. The source voltage (V_S) was chosen to obtain a radiated power in free space equal to 600 mW $(V_S = \sqrt{0.6 \cdot 8 \cdot R_{R0}})$. When analyzing the influence of the metamaterials and the human head on the antenna performance, the source impedance and source voltage were fixed at the Z_S and V_S values. The power radiated from the antenna was evaluated

TABLE II
EFFECTS OF METAMATERIALS ON ANTENNA PERFORMANCES AND SAR
REDUCTION AT 900 MHZ

	$Z_R (\Omega)$	P_R (mW)	Pabs (mW)	SAR_{1g} (W/kg)
No material	$74.59 + j92.75$	600	317.98	2.43
$\mu = 1,\ \varepsilon = -3$	$57.42 + j99.83$	547.3	224.3	1.73
$\mu = 1,\ \varepsilon = -5$	$61.63 - j94.43$	560.9	271.7	2.07

by computing the radiation impedance in this situation ($Z_R = R_R + jX_R$) and used the following [16]:

$$P_R = \frac{1}{2}V_S^2 \frac{R_R}{|Z_R + Z_S|^2}.$$ (5)

The total power absorbed in the head was calculated by

$$P_{\text{abs}} = \frac{1}{2}\int_V \sigma |E|^2 dv.$$ (6)

Different negative medium parameters for SAR reduction effectiveness were analyzed. We placed negative permittivity mediums between the antenna and the human head. First, the plasma frequencies of the mediums were set to be $\omega_{pe} = 11.309 \times 10^9$ rad/s, $\omega_{pm} = 0$ which give mediums with $\mu = 1$ and $\varepsilon = -3$ at 900 MHz. The mediums with larger negative permittivity $\mu = 1$ and $\varepsilon = -5$ were also studied. We set $\Gamma_e = 1.0 \times 10^8$ rad/s, suggesting the mediums have losses. Numerical results of SAR value and antenna performance are given in Table II. The peak SAR_{1g} becomes 1.73 W/kg with $\mu = 1$ and $\varepsilon = -3$ mediums. Compared to the condition without metamaterials, the radiated power is reduced for 8.78% while the SAR is reduced for 28.8%. With the use of $\mu = 1$ and $\varepsilon = -5$ mediums, the SAR reduction effectiveness is decreased. However, the radiated power from the antenna is less affected.

Comparisons of the SAR reduction effectiveness with different positions and sizes of metamaterials were analyzed. Simulation results are shown in Table III. In case A, the distance D between the antenna and metamaterials was changed from 3 mm to 6 mm. In case B, the metamaterials thickness d was reduced from 6 mm to 3 mm. It is found that both the peak SAR_{1g} and power absorbed by the head increase with the increase of distance D or the decrease of thickness d. In case C, the size of metamaterials was increased from 45 mm × 45 to 48 mm × 48 mm. It can be noted that the peak SAR_{1g} is reduced significantly while the degradation on the radiated power due to metamaterials is insignificant.

To further investigate whether the metamaterials less affected the antenna performance or not, radiation pattern of the dipole antenna with $\mu = 1$ and $\varepsilon = -3$ metamaterials were analyzed. The radiation patterns were obtained by the near- and far-field transformation of the Kirchhoff surface integral representation (KSIR) [17]. All the radiation patterns were normalized to the

TABLE III
EFFECTS OF SIZES AND POSITIONS OF METAMATERIALS ON ANTENNA
PERFORMANCES AND SAR VALUES

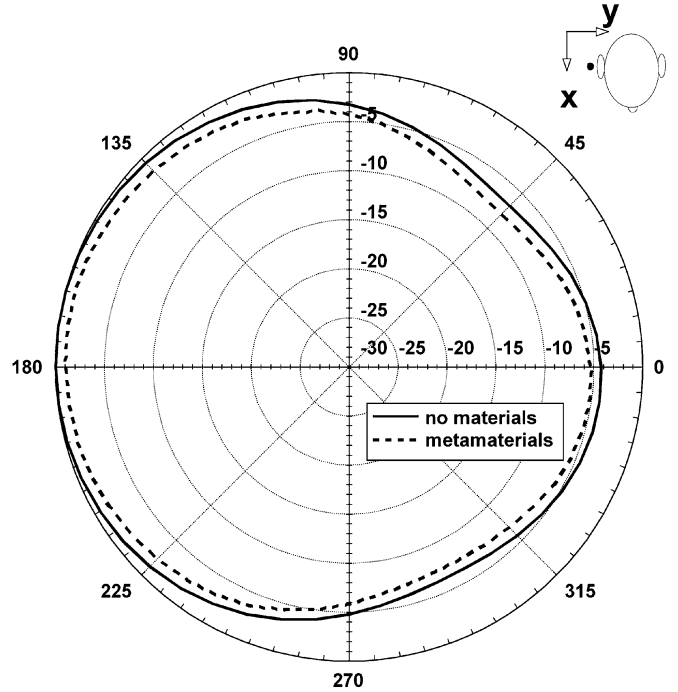|	$Z_R (\Omega)$	P_R (mW)	Pabs (mW)	SAR_{1g} (W/kg)
No material	$74.59+j92.75$	600	317.98	2.43
$\mu = 1,\ \varepsilon = -3$	$57.42+j99.83$	547.3	224.3	1.73
Case A	$65.48+j93.34$	569.4	282.7	2.15
Case B	$73.41+j95.10$	581.5	289.7	2.26
Case C	$83.93+j106.63$	585.4	235.9	1.78

Fig. 3. Calculated ϕ plane radiation pattern at 900 MHz.

TABLE IV
COMPARISONS OF SAR REDUCTION TECHNIQUES WITH DIFFERENT MATERIALS

	$Z_R (\Omega)$	P_R (mW)	SAR_{1g} (W/kg)
$\mu = 1,\ \varepsilon = -3$	$57.42+j99.83$	547.3	1.73
PEC reflector	$71.53+j33.03$	535.61	5.37
Ferrite sheet	$180.34+j161.76$	514.7	0.52

maximum gain obtained without materials. Fig. 3 shows the radiation patterns in ϕ plane for $\theta = 90°$. In [5], the radiation pattern close to the head is reduced about 6 dB and our simulation result is similar to their result. With the use of metamaterials, it can be seen that the maximum degradation of the far field does not exceed 1.21 dB.

The use of metamaterials was also compared with other SAR reduction techniques. The PEC reflector and ferrite material were commonly used in SAR reduction. The PEC reflector and ferrite sheet were analyzed with the same size and position as metamaterials. The relative permittivity and permeability of ferrite sheet were $\varepsilon = 7.0 - j0.58$ and $\mu = 2.83 - j3.25$, respectively. Numerical results are shown in Table IV. A PEC placed between human head and antenna is studied. It can be found that the peak SAR_{1g} is increased with the use of PEC reflector. This is because the EM wave can be induced in the neighbor of a PEC reflector due to scattering. When the size

TABLE V
EFFECTS OF METAMATERIALS ON SAR REDUCTION ($P_{\mathrm{R}} = 0.6$ W FOR 900 MHZ)

	900 MHz	
	No material	$\mu = 1$, $\varepsilon = -3$
SAR_{1g}	2.43	1.89

of PEC sheet is small compared to human head, the head will absorb more EM energy. Similar results of peak SAR increase with PEC placement was also reported in [5]. The use of ferrite sheet can reduce the peak SAR_{1g} effectively. However, the degradation on radiated power from antenna is also significant. In addition, compare to the use of ferrite sheet, the metamaterials can be designed at the desired operation frequency. The metamaterials are designed on circuit board so it may be easily integrated to the cellular phone. The design procedure will be shown in Section III.

To study the effect of SAR reduction with the use of metamaterials, the radiated power from the dipole antenna with $\mu = 1$ and $\varepsilon = -3$ mediums was fixed at 600 mW. Numerical results are shown in Table V. It is found that the use of metamaterials can reduce the peak SAR_{1g} for 22.2%.

From simulation results, the metamaterials can reduce peak SAR effectively and the antenna performances can be less affected. The metamaterials are resonant due to internal capacitance and inductance. The mediums will display a stop band with single negative medium parameter. Besides, we need to be more careful in taking the square root of negative μ and ε of metamaterials. For example, instead of writing $\varepsilon = -3$, we write $\varepsilon = 3\exp(i\pi)$. When the mediums with $\mu = 1$ and $\varepsilon = 3$ are studied, the propagation constant β becomes

$$\beta = \omega\sqrt{\mu\varepsilon\mu_0\varepsilon_0} = \omega\sqrt{3\mu_0\varepsilon_0}\times\exp(i\pi/2) = i\omega\sqrt{3\mu_0\varepsilon_0}. \quad (7)$$

The propagation constant is imaginary and the fields inside the metamaterials will fall off exponentially with the distance from the surface.

III. SRRS DESIGN METHODOLOGY AND SAR REDUCTION

A. SRR Structure

From the FDTD analysis, we found that metamaterials can be used to reduce the peak SAR_{1g} in the head. In this section, the metamaterials operated at 900 and 1800 MHz bands of the cellular phone were designed. The metamaterials can be obtained by arranging SRRs periodically. The SRRs considered here consisted of two square rings, each with gaps appearing on the opposite sides. The configuration has a geometry that is similar to the SRR structures in [18]. As shown in Fig. 4, the structure of a single SRR is defined by the following structure parameters: the square ring size l, the ring thickness c, the ring gap d, and the split gap g. The resonant frequency of SRRs can be shifted toward higher or lower frequency band by properly choosing these structure parameters.

B. SRR Design and Simulation

Numerical simulation can predict the transmission properties of SRRs with various structure parameters. We used FDTD
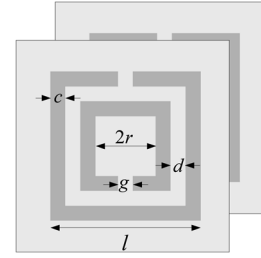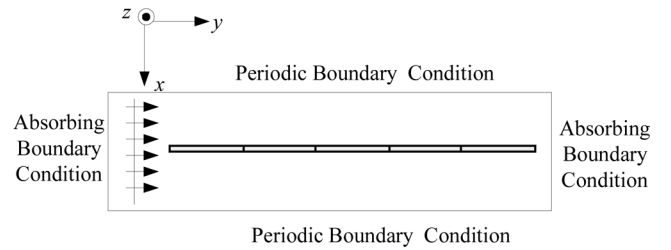

Fig. 4. The structures of SRRs.

Fig. 5. Top view of the FDTD setup for SRRs simulation ($H_\parallel$).
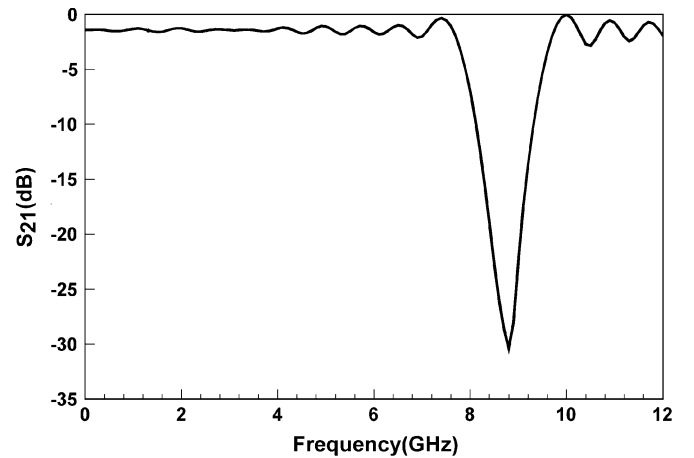

Fig. 6. Modeled transmission spectra of SRRs placed in the yz plane.

method to simulate the SRRs structures. For all simulations, EM wave propagated along the y direction. The electric field polarization was kept along the z axis and magnetic field polarization was kept along x axis. Periodic boundary condition was used to reduce the computational domain and absorbing boundary condition was used at the propagation region. The total-field/scatter-field formulation was used to excite plane wave. The region inside of the computational domain and outside of the SRRs was assumed to be vacuum.

To verify our FDTD simulation, the structure parameters of SRRs were chosen the same as [18]. The structure parameters were $d = g = c = 0.33$ mm, and $l = 3$ mm. The thickness and dielectric constant of the circuit board were 0.45 and 4.4 mm, respectively. The SRRs were placed in the yz plane, as shown in Fig. 5. The unit elements in the propagation y direction were 25 elements. Periodic boundary conditions were applied normal to the propagation direction. Fig. 6 shows the transmission spectra of SRRs in this simulation. In [18], the measured results show that the SRRs display a stop band extending from 8.1 to 9.5 GHz, which is similar to our simulation results.
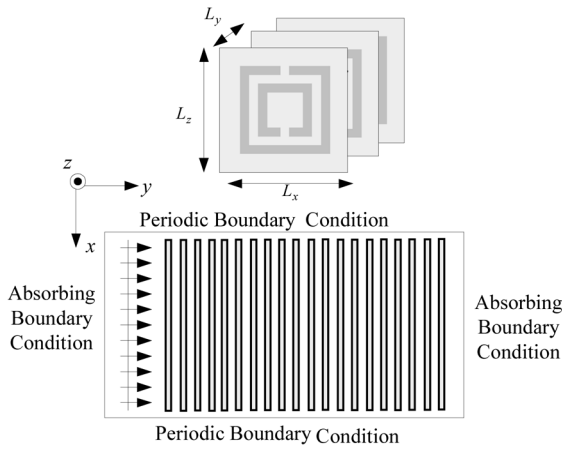
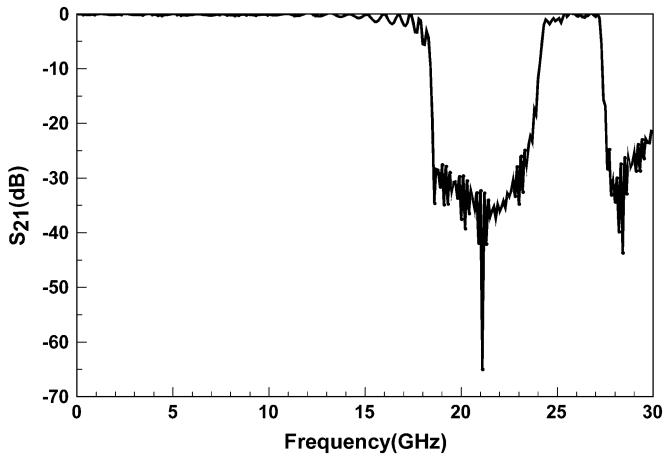Fig. 7. Top view of FDTD simulation for SRRs placed in the xz plane $(H_\perp)$.

Fig. 8. Modeled transmission spectra of SRRs placed in the xz plane.

The SRRs placed in the xz plane were considered, as shown in Fig. 7. The structure parameters of SRRs were the same as previous study in this section. The unit elements in the propagation y direction were 20 elements. Periodic boundary conditions were applied normal to the propagation direction. Fig. 8 shows simulated transmission spectra of SRRs. The stop band is shifted toward higher frequency band and extends from 18 to 24 GHz. From this study, it is found that both of the two incident polarizations can produce stop band. As shown in [19], the stop band corresponds to a region where either permittivity or permeability is negative. When the magnetic field is polarized along the split ring axes $H_\parallel$, it will produce a magnetic field that may either oppose or enhance the incident field. A large capacitance in the region between the rings will be generated and the electric field will be strongly concentrated. There is strong field coupling between SRRs and the permeability medium will be negative at stop band. On the other hand, the behavior of the stop band can be contrasted with that occurring for the $H_\perp$ case. Because the magnetic field is parallel to the plane of SRRs, we assume the magnetic effects are small, and that permeability is small, positive, and slowly varying. In the $H_\perp$ condition, these structures can be viewed as arranging the metallic wires periodically. The continuous wires behave like high-pass filter, which
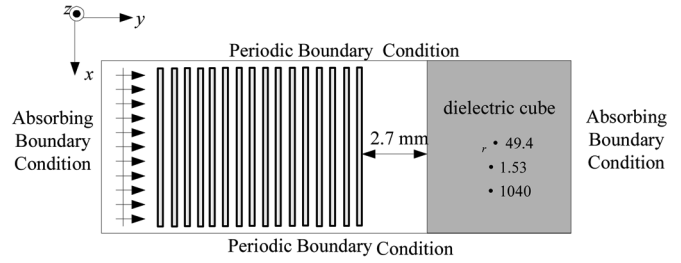

Fig. 9. Top view of FDTD simulation for SRRs with dielectric cube.
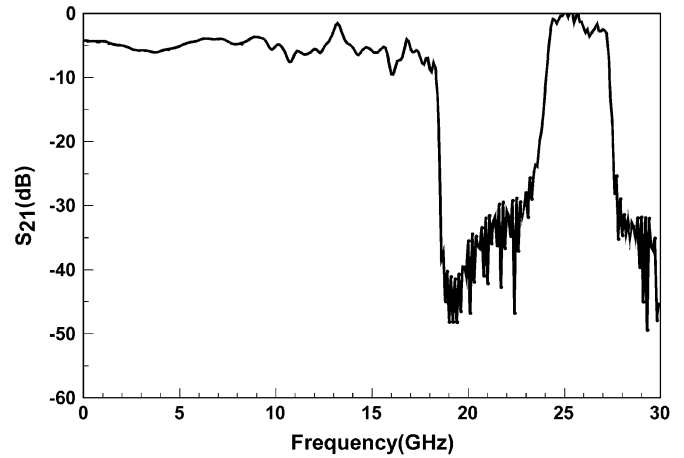

Fig. 10. Modeled transmission spectra of SRRs placed in the xz plane with dielectric cube.

means the permittivity can be negative below the plasma frequency. For this metallic wire structures, there will be a stop band around the resonance frequency. As shown in Fig. 8, a stop band occurs, but outside of the stop band region of the $H_\parallel$ polarization. The contrast between the two stop bands in the $H_\parallel$ and $H_\perp$ cases illustrates the difference between the magnetic and electric responses of the SRRs. Theoretical investigations in [19] have shown that the $H_\parallel$ band gap is due to negative permeability and the $H_\perp$ band gap is due to negative permittivity.

We will investigate whether the performance of metamaterials is affected or not when placing closely to materials with large dielectric constant and conductivity. The SRRs placed closely to dielectric cube with $\varepsilon = 49.4$ and $\sigma = 1.53$ was studied, as shown in Fig. 9. The simulation condition was the same as above study except the presence of dielectric cube. The receiving point of S_{21} is placed between the SRRs and dielectric cube. Fig. 10 shows the calculated transmission spectra of SRRs. Compared to the condition without dielectric cube, the magnitudes of transmission spectra are changed. However, the frequency of stop band is not affected. The SRRs can still retain their propagation properties if placed closely to large dielectric materials.

From the numerical study by FDTD method with Drude model, we find that the peak SAR value in the human head can be reduced by using negative permittivity mediums. The SRRs placed in the xz plane were considered. On the other hand, the size of the metamaterials in the EM propagation direction will not be too large with this placement. To construct the SRRs for SAR reduction, we have changed the structure parameters
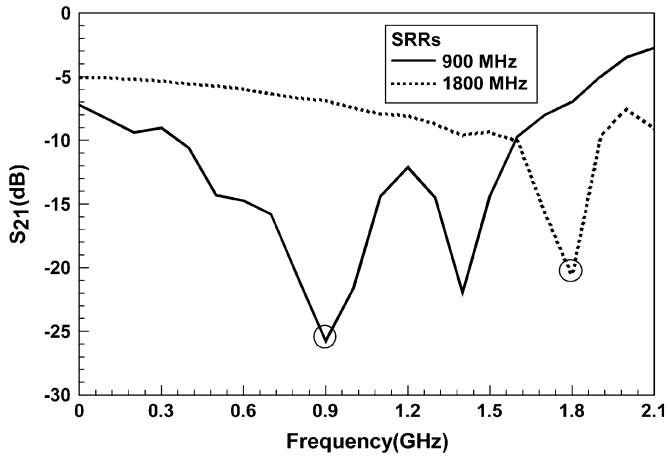
Fig. 11. Modeled transmission spectra of the designed SRRs.

Fig. 12. Structure used in SAR calculation.

of SRRs that the stop band can be designed at 900 and 1800 MHz band, respectively. From FDTD simulation, we found that the ring size l is an important factor for operation frequency. The stop band can be shifted toward lower frequency band by increasing the ring size. To obtain a stop band at 900 MHz, the structure parameters of SRR were chosen as $c = 1.8$ mm, $d = 0.6$ mm, $g = 0.6$ mm, and $l = 43.8$ mm. The periodicity along x, y, z, axes were $L_x = 63$ mm, $L_y = 1.5$ mm, and $L_z = 63$ mm, respectively. On the other hand, to obtain a stop band at 1800 MHz, the structure parameters of SRR were chosen as $c = 1.8$ mm, $d = 0.6$ mm, $g = 0.6$ mm, and $l = 34.2$ mm. The periodicity along x, y, z, axes were $L_x = 50$ mm, $L_y = 1.5$ mm, and $L_z = 50$ mm, respectively. Both the thickness and dielectric constant of the circuit board for operating at 900 and 1800 MHz were 0.508 and 3.38 mm, respectively. The size of the designed SRRs can also be reduced with the use of high dielectric constant circuit board. As shown in Fig. 11, the SRRs medium can display a stop band at 900 and 1800 MHz after properly designing structure parameters.

It is known that a simple frequency selective surface (FSS) can also be used to obtain a stop band. In [20]–[22], a number of FSS are proposed for antenna application. In [22], the authors also proposed CLL structure which is similar to SRR for antenna application. However, these structures display a stop band at several GHz. We have tried to use high impedance surface structure [20] to reduce the peak SAR. However, we found that when these structures are operated at 900 MHz, the sizes of these structures are too large for cellular phone application. A negative permittivity medium can also be constructed by arranging the metallic thin wires periodically [10]. However, we found that when the thin wires are operated at 900 MHz, the size is also too large for practical application. Because the SRR structures are resonant due to internal capacitance and inductance, they are on a scale less than the wavelength of radiation. In this study, it is found that the SRRs can be designed at 900 MHz while the size is similar to that of cellular phone.

C. SAR Calculation in a Muscle Cube

The designed SRRs were used to reduce the SAR value. Since a 3-D model of the whole head with the presence of SRRs struc-
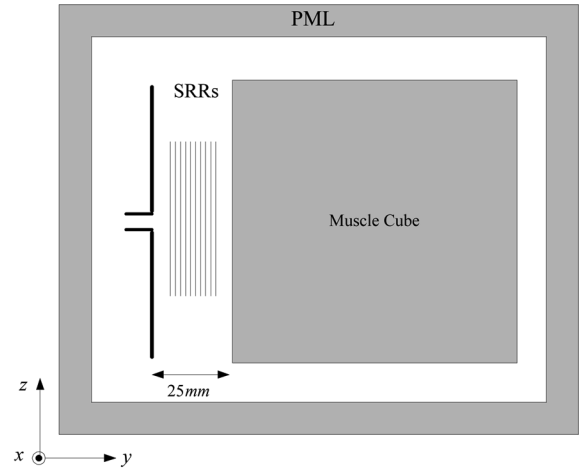
TABLE VI
EFFECTS OF SRRs ON THE ANTENNA PERFORMANCE AND SAR REDUCTION

	900 MHz		1800 MHz	
	No SRRs	With SRRs	No SRRs	With SRRs
Z_R	49.48+j48.81	40.77+j49.04	63.30+j83.26	83.127+j91.88
P_R	600 mW	528.8 mW	125 mW	119.2 mW
SAR_{1g}	8.85	5.59	0.97	0.54

ture requires a great amount of memory in FDTD computation, a simplified muscle cube is studied to validate the effect of SAR reduction. Fig. 12 shows the muscle cube used in SAR simulation. It was formed by muscle tissue with $\varepsilon_r = 51.8, \sigma = 1$, and $\rho = 1040$ at 900 MHz and $\varepsilon_r = 49.4, \sigma = 1.53$ and $\rho = 1040$ at 1800 MHz. The distance between the antenna and the muscle cube was 25 mm. The designed SRRs were placed between the antenna and the muscle cube. The finite sized SRRs with $N_x = 1, N_y = 10$, and $N_z = 1$ unit elements along each direction were considered. The radiated power from the antenna was assumed to be 600 mW at 900 MHz and 125 mW at 1800 MHz, respectively. The size of the muscle cube was chosen equal to the length of the dipole antenna.

The peak SAR_{1g} and antenna performance with SRRs were studied. The results are given in Table VI. The radiated power from the antenna operated at 900 MHz was changed from 600 to 528.8 mW. The peak SAR_{1g} became 5.59 W/kg, a reduction of 36.8% with respect to the condition without SRRs. The antenna operated at 1800 MHz with SRRs was also studied. The radiated power changed to 119.2 mW and the peak SAR_{1g} became 0.54, a reduction of 44.3% with respect to the condition without SRRs. It is found that the radiated power is less affected while the peak SAR_{1g} is reduced significantly with the designed SRRs.

To study the effect of SAR reduction with the use of metamaterials, the radiated power from the dipole antenna with SRRs were fixed at 600 and 125 mW at 900 and 1800 MHz operation bands, respectively. Numerical results of peak SAR_{1g} are shown in Table VII. The peak SAR_{1g} values with SRRs are reduced for 27.57% and 37.62% at 900 and 1800 MHz, respectively. As a consequence, the designed SRRs can be used to re-

TABLE VII
EFFECT OF SAR REDUCTION FOR 900 MHZ AND 1800 MHZ BANDS ($P_R = 0.6$ W FOR 900 MHZ AND $P_R = 0.125$ W FOR 1800 MHZ)

Frequency	No SRRs	SRRs	Reduction %
900 MHz	8.85	6.41	27.57%
1800 MHz	0.97	0.605	37.62%

TABLE VIII
EFFECT OF SAR REDUCTION ON 5% FREQUENCY BANDWIDTH FOR 900 MHZ AND 1800 MHZ

	877 MHz	922 MHz	1755 MHz	1845 MHz
Peak SAR$_{1g}$	5.85	5.24	0.398	0.464

duce the EM interaction between the antenna and the muscle cube.

In general situation, the bandwidth used for mobile communications is 5% or so. The effect of SAR reduction with the designed SRRs on the 5% frequency bandwidth was studied. Table VIII shows the numerical results.

Compared to the peak SAR values without SRRs at 900 and 1800 MHz, the performance of SAR reduction on the 5% frequency bandwidth is also significant.

IV. CONCLUSION

In this work, we have reduced the EM interaction between the antenna and the human head with metamaterials. Based on the 3-D FDTD method with lossy Drude model, it is found that the peak SAR$_{1g}$ in the head can be reduced by placing the metamaterials between the antenna and the human head. The antenna performances can be less affected with the use of metamaterials. Comparisons with other SAR reduction techniques are also demonstrated. We also designed metamaterials from periodically arrangement of SRRs. By properly designing structure parameters, the stop band of SRRs can be designed at 900 and 1800 MHz bands of the cellular phone. The peak SAR$_{1g}$ in a simplified muscle cube with the presence of the designed SRRs is studied and a significant reduction can be obtained. The designed SRRs also have good performance of SAR reduction on 5% frequency bandwidth. Numerical results can provide useful information in designing communication equipments for safety compliance.

REFERENCES

[1] *IEEE Standard for Safety Levels with Respect to Human Exposure to Radio Frequency Electromagnetic Fields, 3 kHz to 300 GHz*, , 1992, IEEE C95.1-1991, Institute of Electrical and Electronics Engineers, Inc. New York.

[2] "Guidelines on limits of exposure to radiofrequency electromagnetic fields in the frequency range from 100 KHz to 300 GHz," *Health Phys.*, vol. 54, no. 1, pp. 115–123, 1988, International Non-Ionizing Radiation Committee of the International Radiation Protection Association.

[3] J. Wang and O. Fujiwara, "FDTD computation of temperature rise in the human head for portable telephones," *IEEE Trans. Microwave Theory Tech.*, vol. 47, no. 8, pp. 1528–1534, Aug. 1999.

[4] C. M. Kuo and C. W. Kuo, "SAR distribution and temperature increase in the human head for mobile communication," in *IEEE-APS Int. Symp. Dig.*, Columbus, OH, 2003, pp. 1025–1028.

[5] J. Wang and O. Fujiwara, "Reduction of electromagnetic absorption in the human head for portable telephones by a ferrite sheet attachment," *IEICE Trans. Commun.*, vol. E80B, no. 12, pp. 1810–1815, Dec. 1997.

[6] A. Hirata, T. Adachi, and T. Shiozawa, "Folded-loop antenna with a reflector for mobile handsets at 2.0 GHz," *Microwave Opt. Technol. Lett.*, vol. 40, no. 4, pp. 272–275, Feb. 2004.

[7] K. H. Chan, K. M. Chow, L. C. Fung, and S. W. Leung, "Effects of using conductive materials for SAR reduction in mobile phones," *Microwave Opt. Technol. Lett.*, vol. 44, no. 2, pp. 140–144, Jan. 2005.

[8] E. Ozbay, K. Aydin, E. Cubukcu, and M. Bayindir, "Transmission and reflection properties of composite double negative metamaterials in free space," *IEEE Trans. Antennas Propag.*, vol. 51, no. 10, pp. 2592–2595, Oct. 2003.

[9] R. W. Ziolkowski, "Design, fabrication, and testing of double negative metamaterials," *IEEE Trans. Antennas Propag.*, vol. 51, no. 7, pp. 1516–1529, Jul. 2003.

[10] M. M. Sigalas, C. T. Chan, K. M. Ho, and C. M. Soukoulis, "Metallic photonic band gap materials," *Phys. Rev. B.*, vol. 52, no. 16, pp. 11744–11751, Oct. 1995.

[11] J. B. Pendry, A. J. Holen, D. J. Robbins, and W. J. Stewart, "Magnetism from conductors and enhanced nonlinear phenomena," *IEEE Trans. Microwave Theory Tech.*, vol. 47, no. 11, pp. 2075–2084, Nov. 1999.

[12] J. N. Hwang and F. C. Chen, "Reduction of the SAR distribution with metamaterials," in *Proc. 16th Asia Pacific Microwave Conf.*, New Dehli, India, 2004, pp. 414–415.

[13] R. W. Ziolkowski and E. Heyman, "Wave propagation in media having negative permittivity and permeability," *Phys. Rev. E.*, vol. 64, pp. 1–15, Oct. 2001.

[14] N. Engheta and R. W. Ziolkowski, "A positive future for double-negative metamaterials," *IEEE Trans. Microwave Theory Tech.*, vol. 53, no. 4, pp. 1535–1556, Apr. 2005.

[15] D. Correia and J. M. Jin, "3-D-FDTD-PML analysis of left-handed metamaterials," *Microwave Opt. Technol. Lett.*, vol. 40, no. 3, pp. 201–205, Feb. 2004.

[16] P. Bernardi, M. Cavagnaro, and S. Pisa, "Evaluation of the SAR distribution in the human head for cellular phones used in a partially closed environment," *IEEE Trans. Electromagn. Compat.*, vol. 38, no. 3, pp. 357–366, Aug. 1996.

[17] O. M. Ramahi, "Near-and far-field calculations in FDTD simulations using Kirchhoff surface integral representation," *IEEE Trans. Antennas Propag.*, vol. 45, no. 5, pp. 753–759, May 1997.

[18] M. Bayindir, K. Aydin, and E. Ozbay, "Transmission properties of composite metamaterials in free space," *Appl. Phys. lett.*, vol. 81, no. 1, pp. 120–122, Jul. 2002.

[19] D. R. Smith, W. J. Padilla, D. C. Vier, S. C. Nemat-Nasser, and S. Schultz, "Composite medium with simultaneously negative permeability and permittivity," *Phys. Rev. lett.*, vol. 84, no. 18, pp. 4184–4187, May 2000.

[20] D. Sievenpiper, "High-impedance electromagnetic surfaces with a forbidden frequency band," *IEEE Trans. Microw. Theory Tech.*, vol. 47, pp. 2059–2074, Nov. 1999.

[21] R. Coccioli, F.-R. Yang, K.-P. Ma, and T. Itoh, "A novel TEM waveguide using uniplanar compact photonic-bandgap (UC-PBG) structure," *IEEE Trans. Microw. Theory Tech.*, vol. 47, pp. 2092–2098, Nov. 1999.

[22] A. Erentok, P. L. Luljak, and R. W. Ziolkowski, "Characterization of a volumetric metamaterial realization of an artificial magnetic conductor for antenna applications," *IEEE Trans. Antennas Propag.*, vol. 53, pp. 160–172, Jan. 2005.

Jiunn-Nan Hwang received the B.S.E.E. and M.S.E.E degrees from National Sun Yat-Sen University, Kaohsiung, Taiwan, R.O.C., in 2000 and 2002, respectively, and is currently working toward the Ph.D. degree at National Chiao Tung University, Hsinchu, Taiwan, R.O.C.

His research interests include the electromagnetic compatibility (EMC)/electromagnetic interference (EMI) problem and computational methods for electromagnetics.

Fu-Chiarng Chen received the B.S. and M.S. degrees from the National Taiwan University, Taipei, Taiwan, R.O.C., in 1988 and 1990, respectively, and the Ph.D. degree from the University of Illinois at Urbana-Champaign, in 1998, all in electrical engineering.

In 1998, he joined the Qualcomm Incorporated, San Diego, CA, where he worked as a Senior Hardware Design engineer on CDMA 3G cellular phones products. Since 2003, he has been an Assistant Professor in the Department of Communication Engineering at National Chiao Tung University. His current research interests include the experimental and computational aspects of applied electromagnetics, antennas, radars, inverse scattering, and RF circuits and systems for wireless communication.

Dr. Chen won the First Place Prize in the 1998 IEEE Antennas and Propagation Society International Symposium Student Paper Competition. He received the Macronix Young Chair Professorship award in 2005.